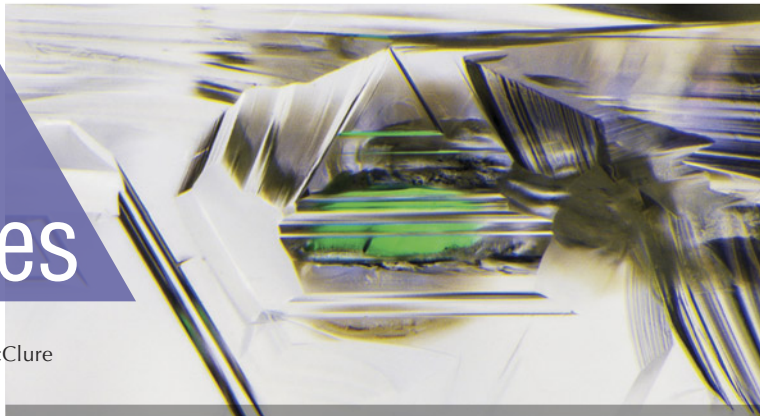


Lab Notes

Editors

Thomas M. Moses | Shane F. McClure



DIAMOND

HPHT-Processed Natural Type Ia Diamond

There are two types of high-pressure, high-temperature processes related to diamond: HPHT treatment and HPHT diamond growth. HPHT laboratory-grown diamonds were developed in the mid-1950s, with the first gem-quality production in the early 1970s and extensive production beginning in the 1990s.

HPHT treatment to change the color of natural diamonds was discovered as a byproduct of annealing natural diamond anvils. The General Electric Company (GE) and Lazare Kaplan International marketed the first commercial HPHT-treated color diamonds in March 1999 (K. Schmetzer, "Clues to the process used by General Electric to enhance the GE POL diamonds," Winter 1999 *G&G*, pp. 186–190). The same machines, such as a hydraulic press that produces extremely high pressure and temperature environments, are also used to treat both mined and laboratory-grown diamonds. HPHT treatment can change the color of diamonds or make them colorless.

A natural 5.20 ct type Ia SI_2 Fancy Dark yellowish brown diamond with natural anhedral crystal inclusions was submitted to the New York labo-

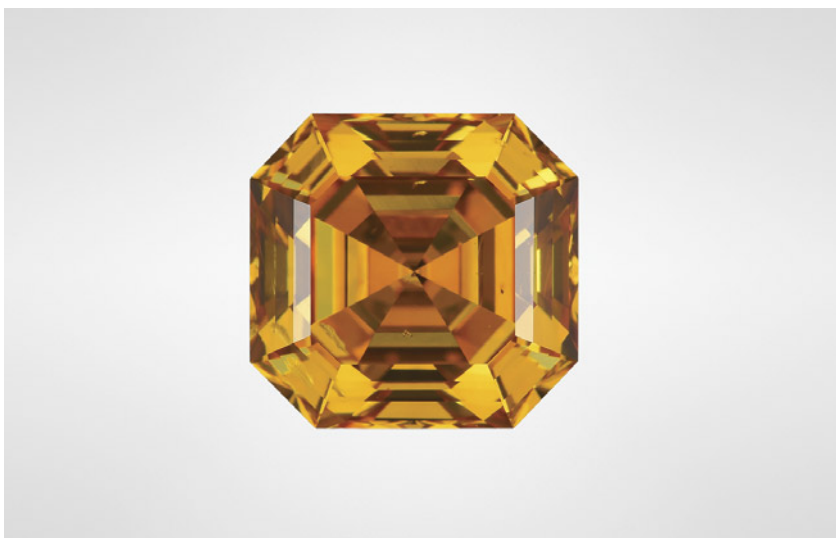


Figure 1. This 5.17 ct Fancy Deep yellow-orange HPHT-treated diamond was resubmitted to the New York laboratory.

ratory for grading services and returned. After being treated, it was resubmitted as a 5.17 ct type Ia SI_2

Fancy Deep yellow-orange diamond (figure 1), with the disclosure that it had been HPHT processed. After

Figure 2. Table-down images showing the diamond before HPHT treatment (left) and after (right).



Editors' note: All items were written by staff members of GIA laboratories.

GEMS & GEMOLOGY, Vol. 58, No. 1, pp. 48–58.

© 2022 Gemological Institute of America

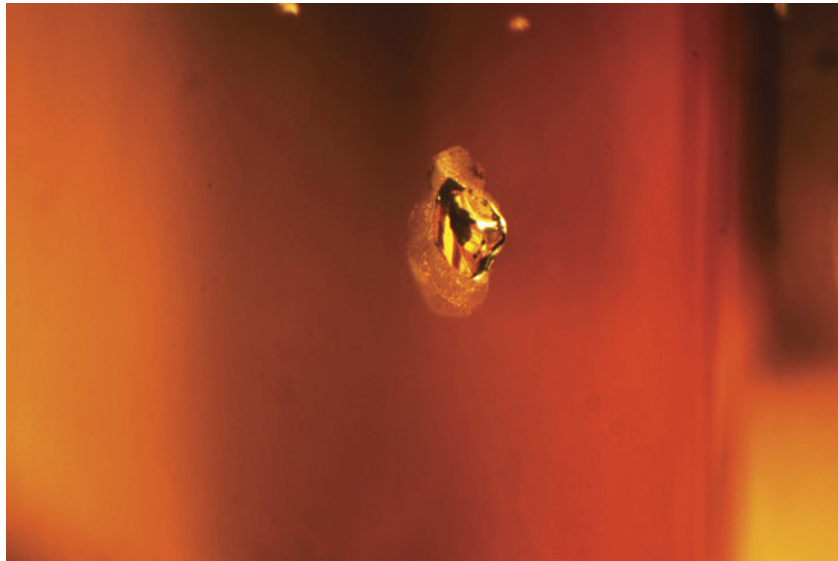


Figure 3. This natural anhedral crystal was formed during diamond growth and acquired a graphitized halo after HPHT treatment. Field of view approximately 1.26 mm.

analysis, the diamond was confirmed to have been treated using an HPHT process that changed the color from a dark yellowish brown to a deep yellow-orange (figure 2). After the HPHT process, each of the natural anhedral crystal inclusions developed a graphitized halo (figure 3). In the natural diamond, the visible/near-infrared (Vis-NIR) absorption spectrum showed a slight 550 nm band—a feature that may impart a pinkish color component depending on its absorbance and other features present within the diamond. After HPHT treatment, there is instead an increase in absorption from ~500 nm toward the lower wavelengths; this absorption rise is due to the creation of single, isolated nitrogen (figure 4).

As expected (I.M. Reinitz et al., “Identification of HPHT-treated yellow to green diamonds,” Summer 2000 *G&G*, pp. 128–137), FTIR data from after the HPHT treatment showed that a peak associated with isolated nitrogen at 1344 cm^{-1} was introduced, the $\sim 1363\text{ cm}^{-1}$ platelet peak was diminished, and the natural amber center at $\sim 4165\text{ cm}^{-1}$ was destroyed (figure 5). Since the spectroscopic data changed after treatment, crystal inclu-

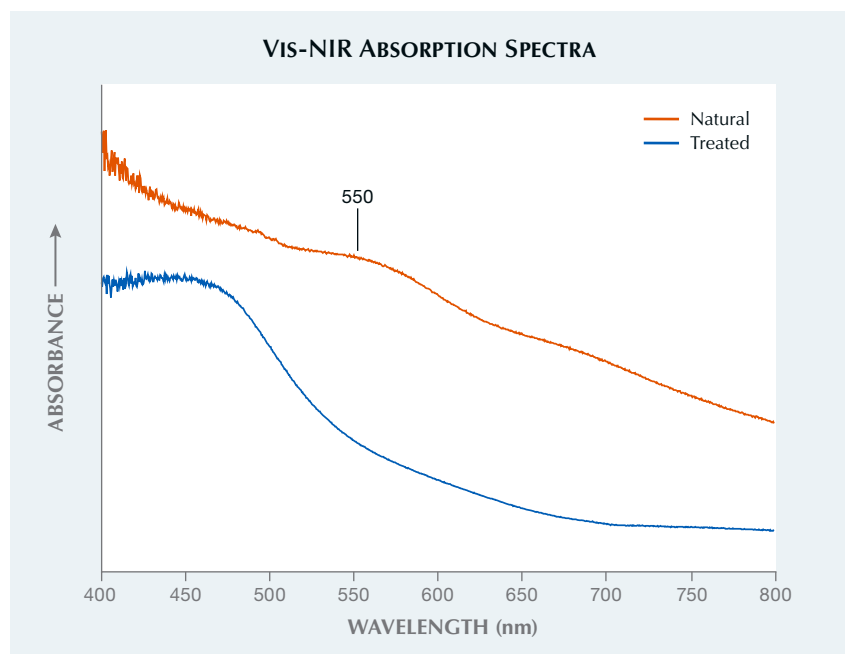
sions plotted on the original grading diagram for this diamond confirmed it was the same stone. The 550 nm band

in the Vis-NIR absorption spectrum related to a pink or brown diamond is stable at lower temperatures of HPHT treatment. Since the 550 nm band was not detected after the process, we believe this diamond was treated at the higher end of the HPHT regime or for a prolonged duration that required repolishing, which caused it to lose three points of carat weight.

While there are many different treatments that can be performed on diamonds, HPHT treatments are permanent and require a stable and controlled environment. In this stone, the treatment resulted in some of the nitrogen aggregates being split apart into single, isolated nitrogen that introduced new color centers and altered the color of the treated stone. The treatment also graphitized inclusions; however, this change was not sufficient to lower the clarity grade. As technology advances, HPHT treatments are becoming more common for both natural and laboratory-grown diamonds.

Sally Ruan

Figure 4. Vis-NIR spectra show the untreated natural diamond with the 550 nm band (orange line). After HPHT treatment (blue line), the 550 nm band is not apparent. Instead, there is an increase in absorption from 500 nm toward the lower wavelengths (higher energy). Spectra are offset for clarity.



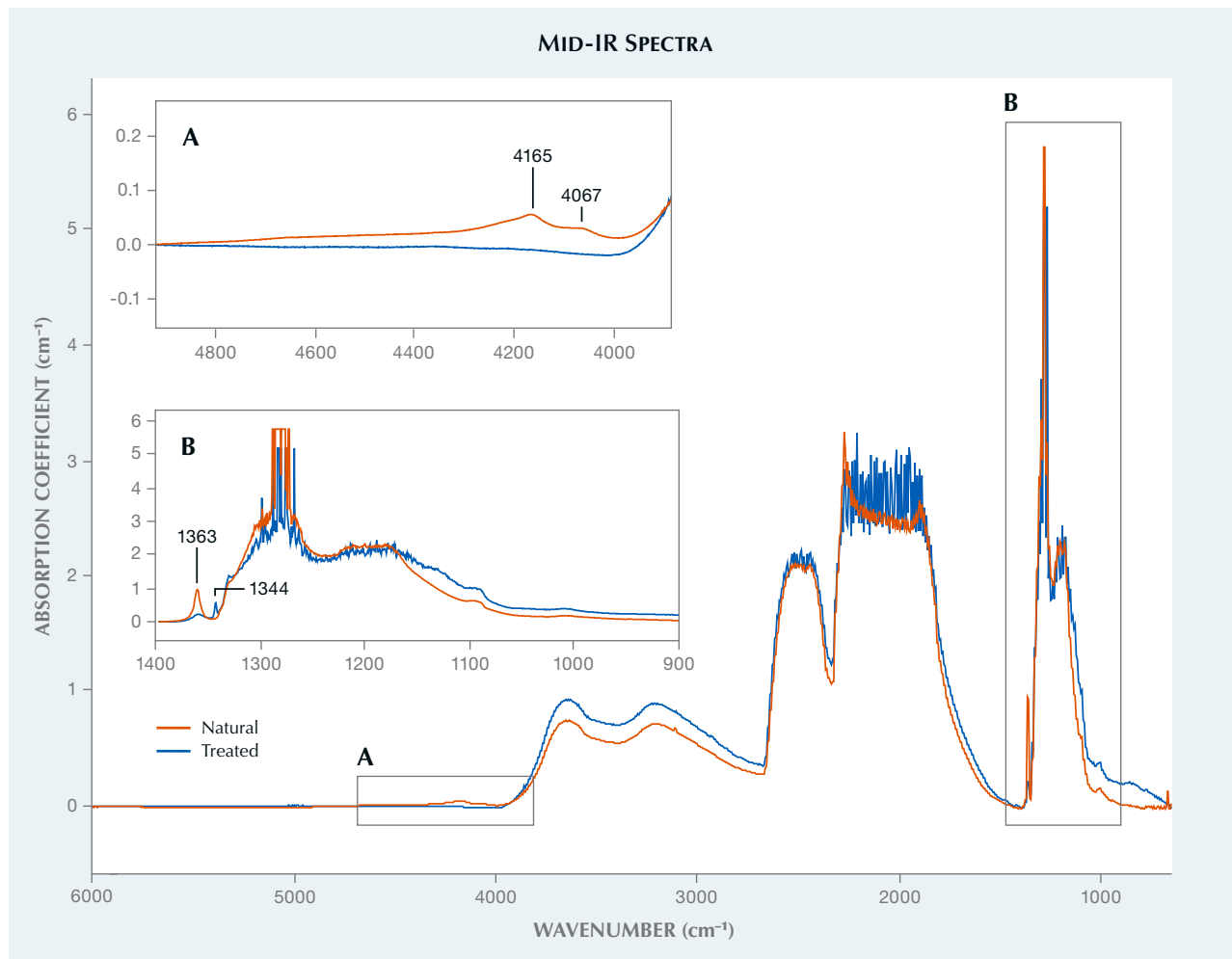


Figure 5. The B region of the mid-infrared spectrum shows a new isolated nitrogen peak at 1344 cm^{-1} and a diminished $\sim 1363 \text{ cm}^{-1}$ platelet peak after HPHT processing (orange line). The A region of the mid-infrared shows that the natural amber center at $\sim 4165 \text{ cm}^{-1}$ (shown in orange) was destroyed after HPHT processing. The spectra are baseline corrected.

Large Green and Yellow Diamonds Colored by Nickel Impurities

Diamonds colored by nickel impurities were previously thought to only occur in lower carat weights and with weaker color saturations. However, the Carlsbad laboratory recently received several large examples with strongly saturated color. Among the stones examined, a Fancy Intense green-yellow cushion weighing 5.02 ct, a Fancy yellow-green pear weighing 5.03 ct, and a Fancy Intense green-yellow pear weighing 5.06 ct were the most notable (figure 6).

Gemologically, these diamonds were mostly free of inclusions except for faint internal graining and small reflective platelets. Along with natural inclusions, FTIR spectra showed that all three stones were type IaA, confirming that these are naturally mined diamonds and not of synthetic origin. Vis-NIR spectra revealed an asymmetrical absorption band around 670 nm and a notable peak at 883 nm for all three (figure 7). These features in the UV-Vis-NIR strongly suggest that the color is caused by the presence of nickel-related defects.

Previously, the largest and most intensely colored gem diamonds reported to have been colored by nickel defects were a 2.54 ct Fancy Light greenish yellow diamond (see Fall 2013 Lab Notes, pp. 173–174) and a 2.81 ct Fancy Intense yellowish green diamond (W. Wang et al., “Natural type Ia diamond with green-yellow color due to Ni-related defects,” Fall 2007 *G&G*, pp. 240–243).

The stones described in the present report are nearly twice as large and have significantly more sat-



Figure 6. Large gem diamonds with strong color saturations resulting from nickel-related impurities. Top: 5.02 ct Fancy Intense green-yellow cushion. Bottom left: 5.03 ct Fancy yellow-green pear. Bottom right: 5.06 ct Fancy Intense green-yellow pear.

urated hues. Therefore, it appears that nickel-colored diamonds can occur over a wider range of sizes and color saturations than previously suspected.

Jamie Price

Nail-Head Spicule in a Russian EMERALD

Recently, a 1.86 ct transparent green pear mixed cut (figure 8) was submitted for identification to the Carlsbad laboratory. Initial testing

Figure 7. Vis-NIR spectra collected from each diamond show a strong asymmetrical absorption band around 670 nm along with a distinct peak at 883 nm. These defects together, with the lack of any other color-causing defects, indicate that nickel is the main cause of color.

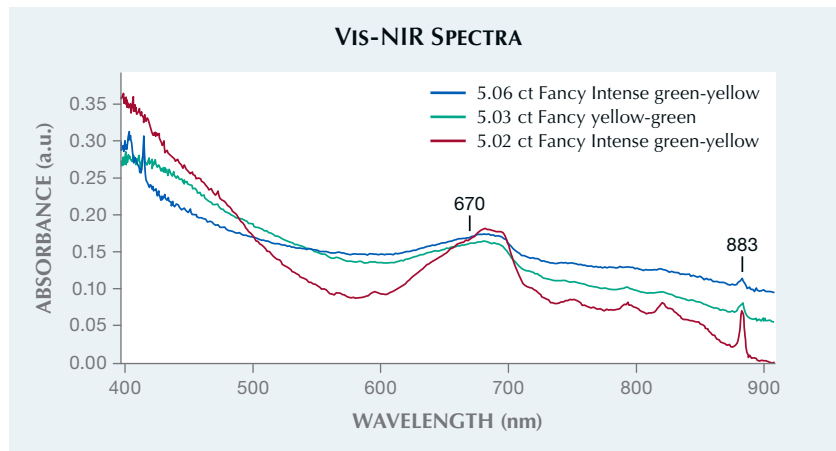


Figure 8. A 1.86 ct transparent green pear mixed-cut emerald.

produced the following results: refractive index values of 1.582–1.590, birefringence of 0.008, doubly refractive, and a hydrostatic specific gravity of 2.73. The long-wave UV reaction was red with a blue fluorescence in surface-reaching fractures from the clarity enhancement. These results were consistent with natural emerald. Trace element chemistry of the host emerald collected via laser ablation–inductively coupled plasma–mass spectrometry (LA-ICP-MS) matched well with GIA’s Russian emerald chemistry reference data.

While the identification of any gem requires further testing with a variety of instruments, in most cases the stone’s natural or synthetic origin can be determined conclusively by features seen under magnification. Nail-head spicules are typically associated with synthetic hydrothermal (and occasionally flux-grown) emerald and synthetic quartz, but they are also occasionally found in natural gems such as beryl, sapphire, spinel, tourmaline, and quartz (G. Choudhary and C. Golecha, “A study of nail-head

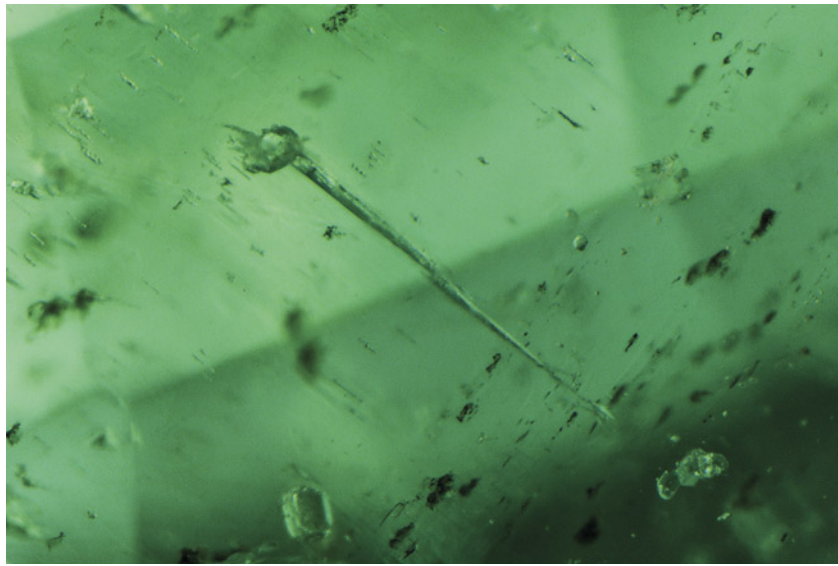


Figure 9. Nail-head spicule in the natural emerald from figure 8. Field of view 2.01 mm.

spicule inclusions in natural gemstones," Fall 2007 *G&G*, pp. 228–235; K. Schmetzer et al., "Multicomponent inclusions in Nacken synthetic emeralds," *Journal of Gemmology*, Vol. 26, No. 8, 1999, pp. 487–500).

Nail-head spicules are wedge-shaped two-phase (liquid and gas) inclusions capped by crystals that act as growth obstacles (figure 9). During growth of the host crystal, a small crystal or platelet is deposited on its surface. As

the crystal continues to grow past the inclusion, a tapered void is created, which traps the hydrothermal growth medium such that, upon cooling, it becomes two phases consisting of liquid and a gas bubble (Choudhary and Golecha, 2007).

Maxwell Hain

Dyed FLUORITE

Two pieces of green rough weighing 358.03 and 454.27 ct (figure 10) were recently sent to the Carlsbad laboratory for an emerald identification and origin report. Standard gemological testing could not be performed due to the rough surfaces and size of the stones. Raman spectroscopy was used to aid in the identification (figure 11), and the Raman spectra were consistent with the mineral fluorite.

Internally and externally, both pieces showed typical massive habit fluorite features. Small octahedral crystals were scattered along the surfaces, and perfect cleavage in four di-

Figure 10. These two rough pieces weighing 454.27 and 358.03 ct were identified as dyed fluorite.



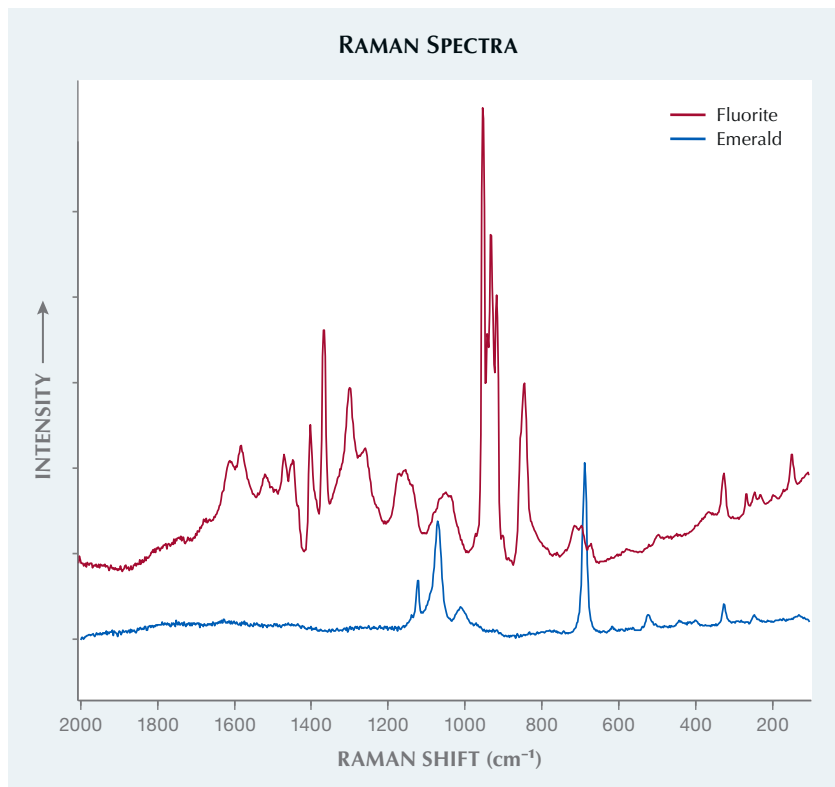
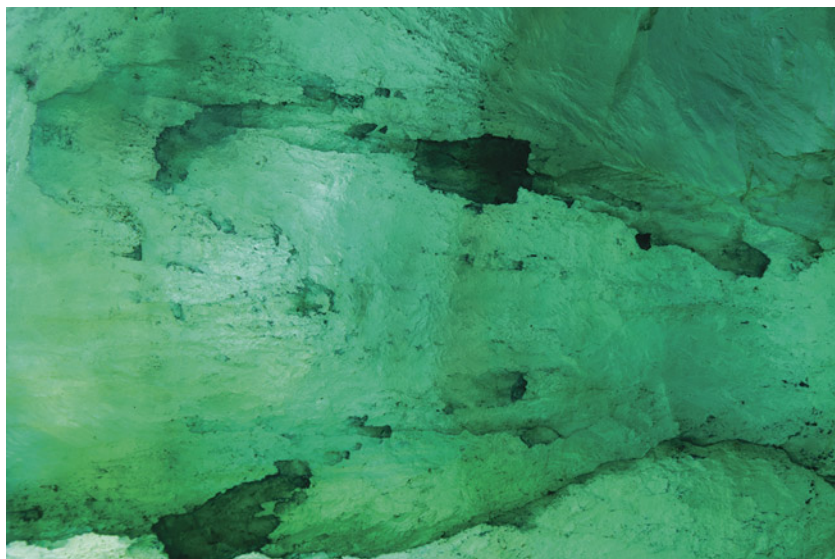


Figure 11. Overlay of the Raman spectra of one of the dyed fluorite samples and a known emerald sample.

rections was documented. Cleavage is not a gemological property of emerald, and octahedral cleavage is a key identifying feature for fluorite. Weak

color banding could be seen with diffused lighting, but the most abnormal observation with both of these stones was the presence of obvious dye con-

Figure 12. Obvious dye concentrations within surface-reaching fractures. Field of view 7.26 mm.



centrations along their fractures (figure 12).

Fluorite naturally comes in a wide range of colors and can have multiple colors in a single crystal. These stones are a careful reminder to analyze every stone thoroughly for proper identification and to detect the most uncommon of treatments.

Nicole Ahline

Repaired GRANDIDIERITE

Recently the Carlsbad laboratory received for identification services a transparent bluish green stone weighing 1.43 ct and measuring $7.47 \times 6.31 \times 4.06$ mm (figure 13). Standard gemological testing revealed a refractive index of 1.58–1.62 on both the crown and pavilion, suggesting that both the crown and pavilion were grandidierite. This was confirmed using FTIR and Raman spectroscopy. Microscopic examination showed a very large fracture that broke continuously around the entire stone. Closer inspection revealed that the fracture was filled (figure 14), and this filling was holding the stone together, indicating that the stone was likely broken into two pieces and then repaired with a resin or glue.

Figure 13. Flattened gas bubbles caught in the break of a filled fracture are visible face up in this 1.43 ct repaired grandidierite.





Figure 14. Flattened gas bubbles caught in the filling of the large fracture that breaks continuously through the entire pavilion and some of the crown. Field of view 4.79 mm.

Grandidierite is a very rare mineral, and transparent gem-quality material was not found in the market until 2015 (Winter 2015 Gem News International, pp. 449–450). Named after French naturalist Alfred Grandidier (1836–1912), grandidierite was first discovered in 1902 at the cliffs of Andrahomana on the southern coast of Madagascar (D. Bruyere et al., “A new deposit of gem-quality grandidierite in Madagascar,” Fall 2016 *G&G*, pp. 266–275). This is the first repaired grandidierite GIA has seen to date.

Michaela Stephan

LABORATORY-GROWN DIAMOND New Record Size for CVD Laboratory-Grown Diamond

Growth technology of single-crystal diamond has advanced significantly in the last two decades for both the high-pressure, high-temperature (HPHT) and chemical vapor deposition (CVD) methods. In addition to many other applications, laboratory-grown diamonds have become an expanding segment of the jewelry industry. Records for crys-

tal size and quality are frequently broken. In this note, GIA's New York laboratory reports on a new record for CVD laboratory-grown diamond.

This square modified brilliant diamond produced by Shanghai Zhengshi Technology Co. Ltd. (figure 15) weighed 16.41 ct and measured 13.97 × 13.87 × 9.56 mm, with G color and VVS₂ clarity. The strong graining distributed throughout it created a “wavy” appearance (see the video at www.gia.edu/gems-gemology/spring-2022-lab-notes-new-record-size-CVD). In addition, a few tiny pinpoints were present. Absorption spectroscopy in the infrared region revealed this was a typical type IIa diamond. Except for absorptions from the diamond itself, no other defect-related absorption was detected in this region. Photoluminescence spectroscopy collected at liquid nitrogen temperature with 514 nm laser excitation (figure 16, left) showed emissions from NV centers with zero-phonon lines (ZPL) at 575.0 and 637.0 nm with moderate intensities. Clear emissions from SiV⁰ at 736.6 and 736.9 nm were detected. Weak emissions at 596 and 597 nm, which are specific to CVD diamond and also unstable at high temperature, were recorded overlapping with sidebands of the NV⁰.

Figure 15. The new record size for CVD laboratory-grown diamond—16.41 ct, with G color and VVS₂ clarity—has been achieved by Shanghai Zhengshi Technology Co. Ltd. This is an as-grown diamond; no post-growth treatment was applied for color improvement, either before or after faceting.



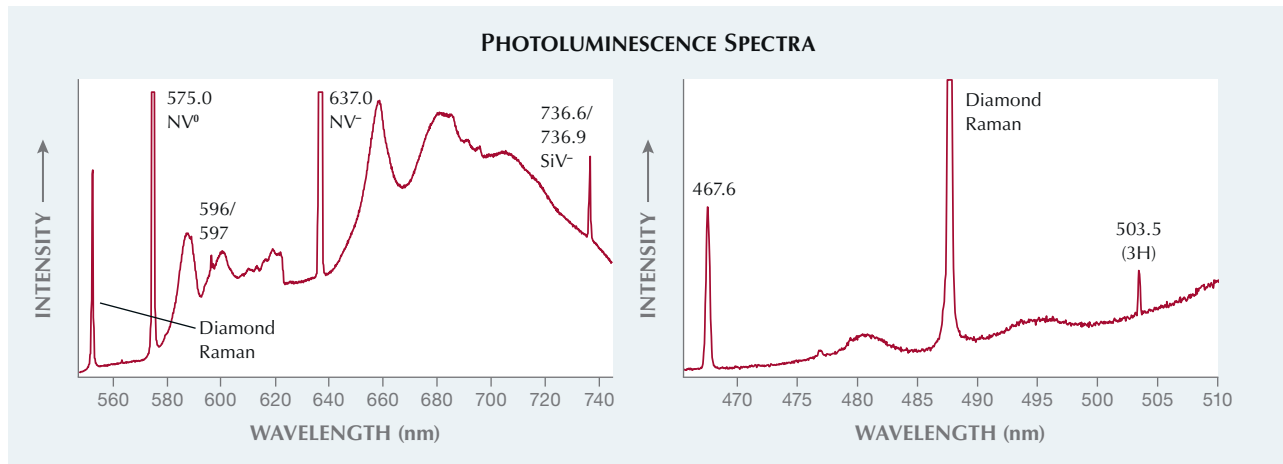
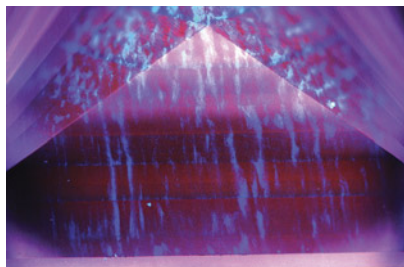


Figure 16. Left: The photoluminescence spectrum with 514 nm laser excitation under liquid nitrogen temperature showed typical features of as-grown CVD diamond. Right: In the photoluminescence spectrum with 457 nm laser excitation under liquid nitrogen temperature, weak emissions from the 3H defect and from the 467.6 nm center were recorded.

Photoluminescence spectroscopy with 457 nm laser excitation (figure 16, right) detected weak emissions at 503.5 nm (3H) and 467.6 nm. Similar to the emission at 596 and 597 nm, the 467.6 nm center is CVD-specific and would be annealed out at very high temperature. No emission from the H3 defect was observed. All these spectroscopic features confirmed this was a CVD diamond with no post-growth treatment to improve the color.

Images collected under deep short-wave UV excitation showed strong orange-red fluorescence with banded

Figure 17. Fluorescence imaging with deep short-wave UV excitation showed the typical orange-red fluorescence of as-grown CVD diamond with irregular blue “banding.” Up to seven growth layers were revealed.

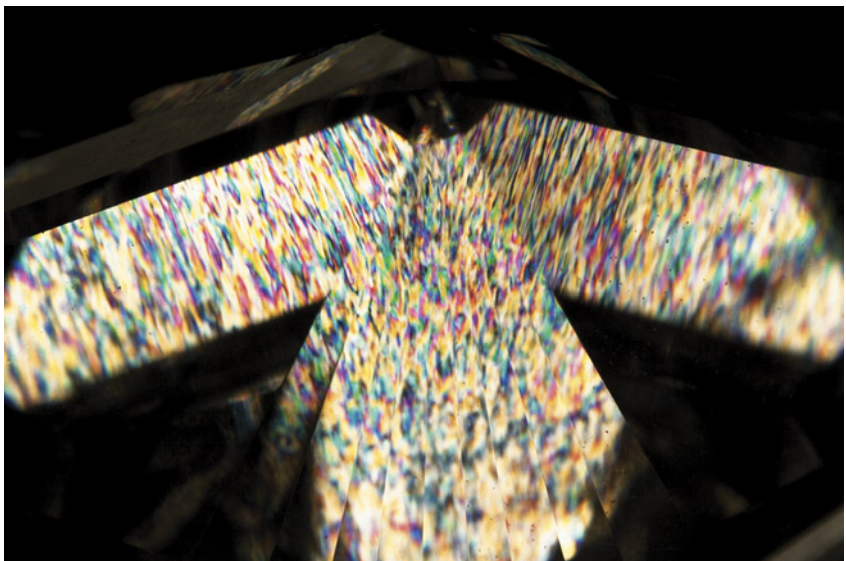


blue regions (figure 17). The blue “columns” were nearly perpendicular to the table and extended almost continuously to the pavilion and culet. This feature was consistent with both the strong lattice dislocations observed under the microscope with crossed polarizers (figure 18) and its observable graining. Up to seven growth steps were revealed in the fluorescence and cathodoluminescence images (figure 19), with each layer of

similar thickness. This square modified brilliant diamond was faceted with its table face parallel to these layers for maximum weight retention, while keeping excellent proportions and symmetry.

For CVD growth, this 16.41 ct diamond broke the record previously held by a 14.60 ct diamond (emerald cut, F color, VS₂ clarity) produced in India, which surpassed the previous record of 12.75 ct (round brilliant, F

Figure 18. The large CVD diamond showed very strong dislocations under crossed polarizers, the main cause of its wavy appearance.



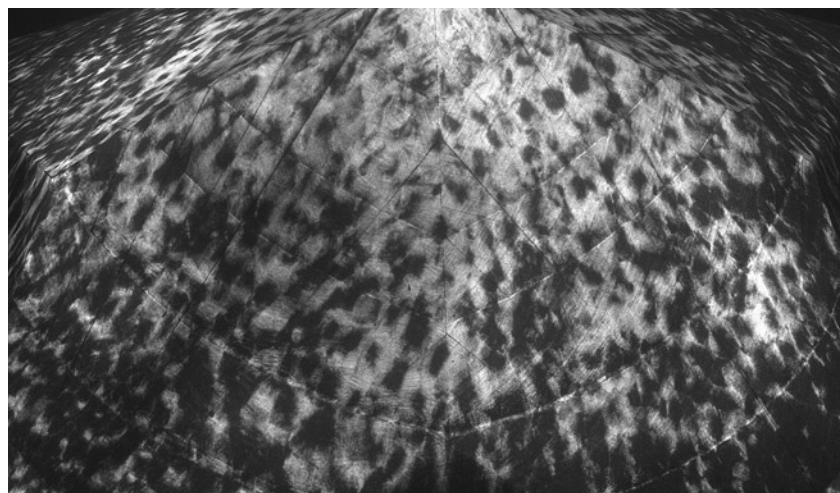


Figure 19. Cathodoluminescence imaging also revealed the seven growth steps. The dark dots in this image are related to the lattice dislocations.

color, VVS₂ clarity), both reported last year (“IGI certifies world record 14.60 ct lab grown diamond,” *IGI Gem-Blog*, August 31, 2021). In comparison, the largest colorless or near-colorless HPHT laboratory-grown diamond is 15.32 ct (cushion cut, H color, I₁ clarity); see Summer 2018 Lab Notes, pp. 217–218. The largest laboratory-grown diamond of any kind tested by GIA so far is a 20.23 ct cushion cut (Fancy Vivid yellowish orange, VS₂) produced using the HPHT method in 2019. GIA will continue to follow the development of laboratory-grown diamonds to ensure that all are properly identified.

Wuyi Wang, Stephanie Persaud, and
Elina Myagkaya

Unusual Laser Drill Holes in a Laboratory-Grown Diamond

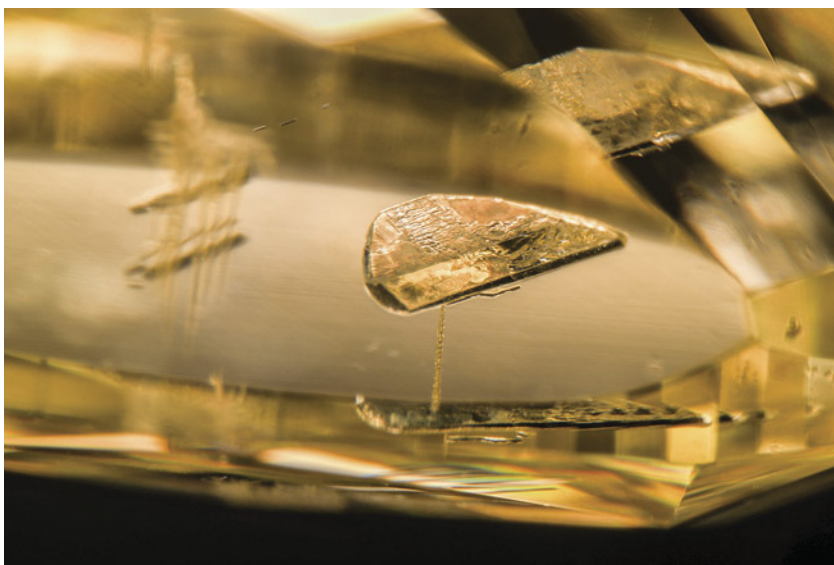
Diamonds with dark inclusions have been laser drilled to enhance their clarity for more than 60 years. The internal inclusion is drilled from the diamond surface and then acid-boiled to bleach it out. GIA has identified many natural diamonds treated by this technique, but the Carlsbad laboratory recently received for a colored diamond identification and origin report an undisclosed laboratory-grown diamond with unusual laser drill holes.

The diamond was a Fancy yellow cushion modified brilliant weighing 2.02 ct. Gemological and spectroscopic analysis confirmed it was an HPHT-grown synthetic diamond. The diamond was attracted to a small magnet due to the numerous metallic inclusions. No strain was visible under crossed polarizers, and DiamondView imaging showed the typical cuboctahedral HPHT growth pattern.

Clarity was low due to the presence of numerous large flux inclusions, so laser drilling was likely done to enhance the appearance and clarity. One of the laser drill holes connected to a large flux inclusion can be seen in figure 20. A metallic flux inclusion cannot be bleached as some mineral inclusions can and so it must be dissolved out, which could pose additional challenges to improving the clarity. It appears there was an unsuccessful attempt to remove the flux, as the inclusion was still eye visible.

Three clusters of intersecting laser drill tubes resembling corals were observed (figures 21 and 22). We could see numerous roundish openings on the surface filled with dark materials. Raman spectroscopy confirmed they were all non-diamond carbon materials. Here the laser beam was likely reflected off a flux inclusion and refocused to a new point farther than intended, resulting in the unusual branching pattern. Other flux inclusions could have been successfully dissolved by acid because they were smaller than the one in figure 20 or because there were more drilled tubes for the acid to enter. This may have

Figure 20. Flux inclusion in a laboratory-grown diamond connected to a laser drill hole. Field of view 3.57 mm.



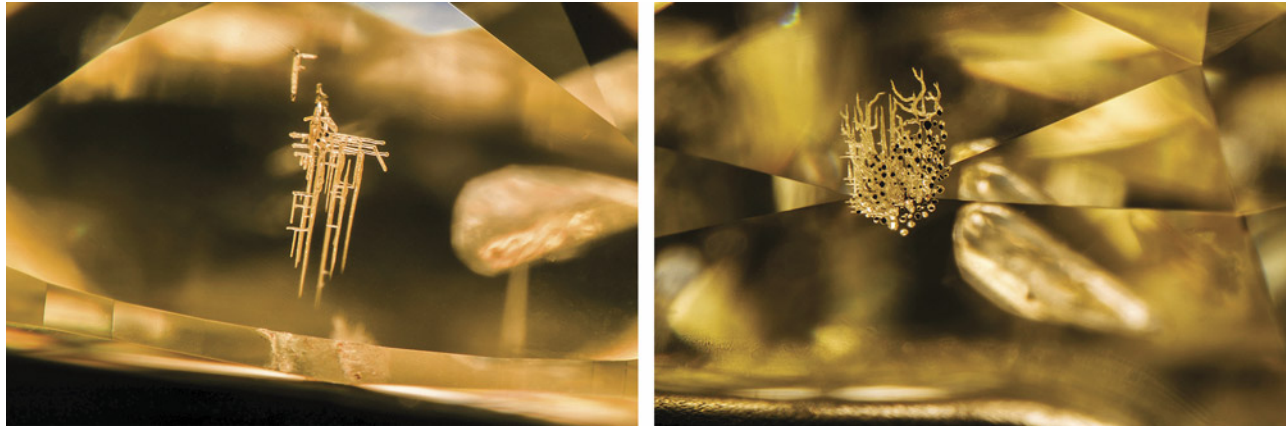


Figure 21. Clusters of unusual laser drill holes in a laboratory-grown diamond. Fields of view 3.57 mm (left) and 2.61 mm (right).

caused the unique crossed tubes inside the stone. Burn marks on the surface next to some of the laser drill holes might have been due to the heat generated by the laser beam (figure 22).

This diamond was identified as a laboratory-grown diamond. It was issued a laboratory-grown colored diamond report stating, "Laser drill holes are present."

Najmeh Anjomani and Troy Ardon

Hydrothermal SYNTHETIC RUBY

Hydrothermal synthetic ruby was first introduced to the market in the 1960s (A. Peretti and C.P. Smith, "An in-depth look at Russia's hydrothermal synthetic rubies," *JewelSiam*, April-May 1993, pp. 96–102). The hydrothermal process is very slow and requires high heat and very high pressure (400–600°C, 5,000–30,000 psi), mimicking the conditions deep in the earth that result in the formation of natural ruby. In this method, the corundum seed plates are suspended inside the growth chamber and nutrients are placed in the bottom. Slowly the nutrients dissolve and form a solution which deposits new synthetic corundum growth onto the seed crystal. The size of the synthetic crystal depends on the size of the seed, amount of nutrient solution, and time.

The Carlsbad laboratory recently received a 4.55 ct transparent cushion-cut hydrothermal synthetic ruby for an identification report (figure 23). This type of laboratory-grown ruby is seldom submitted to the laboratory today, though they were more prevalent in the 1980s. Gemological testing yielded an RI of 1.761–1.769 and a specific gravity of 3.99. Its fluorescence reaction was strong red to long-wave and medium red to short-wave

UV radiation, and its pleochroism was orangy red to purplish red. These properties are typical of most rubies, natural or laboratory grown.

Chemical analysis was done by EDXRF and showed a high amount of chromium (1550 ppma), low iron (153 ppma), titanium (25.5 ppma), no gallium, and very low vanadium (2.24 ppma), which matches the synthetic corundum chemistry.

Magnification showed characteris-

Figure 22. Burn mark on the surface next to laser drill holes. Field of view 2.01 mm.



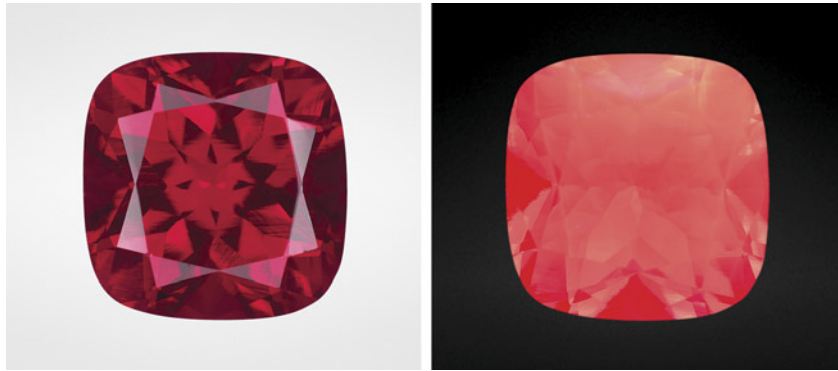
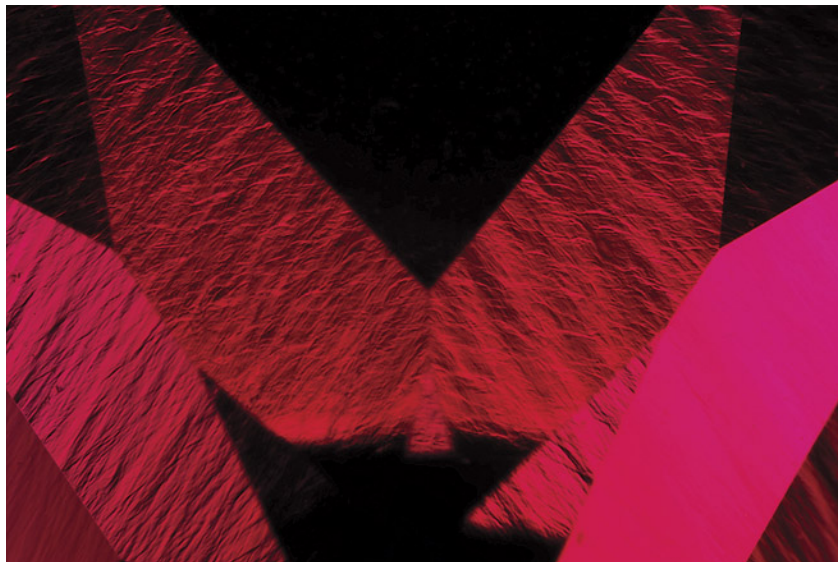


Figure 23. Photos of the hydrothermal synthetic ruby in daylight and short-wave UV light.

tic internal features of hydrothermal synthetic corundum such as subparallel striations and angular/zigzag (chevron) graining using a standard gemological microscope in conjunction with fiber-optic light or diffused light (figure 24).

Figure 24. The chevron growth structure observed in the hydrothermal synthetic ruby. Field of view 4.79 mm.



The baseline-corrected spectra showed very strong water peaks in the region between 3200 and 3600 cm^{-1} , which is strongly indicative of hydrothermal synthetic origin. (The instrument was baseline corrected to remove the water signal from the at-

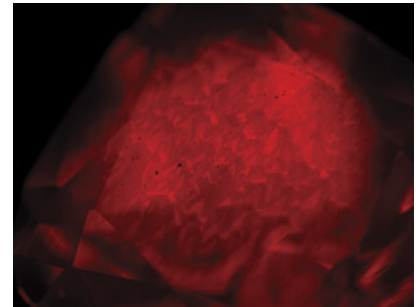


Figure 25. The DiamondView image of the chevron growth pattern in the hydrothermal synthetic ruby. Field of view 8.63 mm.

mosphere as well as having the sample chamber purged with dry air to minimize the detection of water from the atmosphere.) Luminescence images in an ultra-short-wave UV radiation DiamondView showed an interesting chevron growth pattern as well with red fluorescence, further confirming hydrothermal synthetic origin (figure 25).

While hydrothermal synthetic rubies are not as common in the gem trade today, it is helpful to review the distinctive features and characteristics that make them identifiable.

Shiva Sohrabi and
Najmeh Anjomani

PHOTO CREDITS

Towfiq Ahmed—1, 15; Sally Ruan—3; Diego Sanchez—6, 8, 23; Nathan Renfro—9; Annie Haynes—10, 13; Nicole Ahline—12; Michaela Stephan—14; Stephanie Persaud—17, 18; Elina Myagkaya—19; Najmeh Anjomani—20–22; Shiva Sohrabi—24, 25